MOLECULAR DYNAMIC SIMULATION STUDY OF MELTING POINT OF L12-Cu_3Au ALLOY

Murat CELTEK[1] and Unal DOMEKELI[2]
[1]*Faculty of Education, Trakya University, Edirne, Turkey*
[2]*Faculty of Science, Trakya University, Edirne, Turkey*

Abstract
In this study, the melting point and specific heat of L12-Cu3Au alloy was investigated by classical molecular dynamic simulation method using three different many-body potentials. Simulation box contains 15×15×15 unit cells with 13500 atoms, periodic boundary conditions are applied in three directions. All simulations were performed using DLPOLY molecular dynamic open code. The solid-liquid phase transition was investigated by analyzing the lattice parameters, pair distribution function and specific heat as a function of temperature. The results of molecular dynamics simulation obtained using different potentials were discussed comparatively with the experimental and theoretical results reported in the literature.

Keywords: molecular dynamics simulation, melting point, specific heat, solid-liquid phase, pair distribution function.

INTRODUCTION

As a traditional alloy, Au-Cu alloy systems are widely used in many fields such as catalysis, electronics industries and biological materials. The interest in these alloys is increasing day by day, and in recent studies, some new functions of the alloy have been found in nano-crystal and thin film materials[1–4]. Molecular dynamics (MD) is the simulation of the physical movement of atoms and molecules. The atoms and molecules are allowed to interact for a time that gives an image of the movement of atoms. The equations of motion are solved numerically to follow the time evolution of the system, allowing the derivation of kinetic and thermodynamic properties[5]. Optimal identification of atomic interactions in the system is very important in terms of the reliability of the potential function used. In this context, there are several potential functions used in molecular dynamic simulation such as Lennard Jones (LJ), Embedded Atom Method (EAM), Modified Embedded Atom Method (MEAM), Quantum Sutton-Chen (Q-SC)[6], Tight-Binding (TB)[7], Tersoff [8], which are used in different systems depending on the application.

In our study, we examined the physical properties of the Cu_3Au (or $Cu_{75}Au_{25}$) binary alloy during the heating process by using many-body potentials such as EAM, Q-SC and TB among the aforementioned potential functions. The results obtained from MD simulation were discussed by comparing with the experimental and theoretical results presented in the literature.

EXPOSITION

At the beginning of the MD simulation study, Cu and Au atoms in the alloy system were distributed to fcc unit cell-based L12 type super braid points. The Au atoms occupy the corner sites, whereas the Cu atoms occupy the face centers of the basis cube. The simulation system consists of 13500 atoms (10125 Cu atoms and 3375 Au atoms), and is confined in a cubic simulation cell with periodic boundary conditions imposed in all three directions. The Nosé-Hoover thermostat and barostat has been used to control the temperature and pressure[9]. For all three potentials, the simulations start from a well equilibrated state initiated by a perfect L12 configuration at 0K. The output configurations of the simulation run at each temperature

provide the starting point for the next temperature. The system was heated from 0K to 1800K at 50K intervals. In order to better determine the melting point, computer simulations have been carried out by 10K increments around the melting point.

The total energy forms of the Q-SC, EAM and TB many-body potentials used in the study are given as follows, and more detailed information about these potentials can be taken from the relevant references.

Total energy in the potential of Q-SC has the following form[10,11]:

$$U_{tot} = \sum_{i}^{N} \left[\sum_{j \neq i} \mathsf{T}_{ij} \frac{1}{2} \left(\frac{a_{ij}}{r_{ij}} \right)^{n_{ij}} - c_i \mathsf{T}_{ii} \left(\sum_{i \neq j} \left(\frac{a_{ij}}{r_{ij}} \right)^{m_{ij}} \right)^{1/2} \right] \quad (1)$$

The Q-SC potential parameters used for the Cu-Au alloy are presented in Table 1[6,10].

Table 1. *Q-SC potential parameters for the Cu and Au pure metals.*

Metal	n	m	ϵ (eV)	c	a (Å)
Cu	10	5	5.7921E−3	84.843	3.6030
Au	11	8	7.8052E−3	53.581	4.0651

In the second-moment approximation (SMA), the total energy of the TB potential can be written as follows [12,13]:

$$E = -\sum_{i=1}^{N} \left(\sum_{j \neq i} A_{\alpha\beta} \exp\left[-p_{\alpha\beta} \left(\frac{r_{ij}}{r_0^{\alpha\beta}} - 1 \right) \right] - \left\{ \sum_{j \neq i} \xi_{\alpha\beta}^2 \exp\left[-2q_{\alpha\beta} \left(\frac{r_{ij}}{r_0^{\alpha\beta}} - 1 \right) \right] \right\}^{1/2} \right) \quad (2)$$

In this study, we used the potential parameters of TB obtained by Papanicolaou et al.[14] and listed these parameters in Table 2.

Table 2. *TB potential parameters for the Au-Au, Cu-Cu and Cu-Au.*

$\alpha\beta$	$\xi_{\alpha\beta}$ (eV)	$A_{\alpha\beta}$ (eV)	$q_{\alpha\beta}$	$p_{\alpha\beta}$	$r_0^{\alpha\beta}$ (Å)
Au–Au	1.8241	0.2145	4.3769	10.8842	2.8652
Cu–Cu	1.2355	0.0862	2.3820	12.5785	2.4729
Cu–Au	1.7981	0.2356	2.6433	8.6961	2.6222

We used the EAM potential developed by Zhou and his co-workers [15] to describe the interactions between Cu and Au in Cu_3Au binary alloy. In the EAM potential, the total energy is written as the sum of the embedding energy and the pair potential, and given in the following form[16–18].

$$E_i = F_i(\rho_{h,i}) + \sum_i \sum_j \varphi_{ij}(r_{ij}), \quad (3)$$

$$\rho_{h,i} = \sum_{j \neq i} f_j(r_{ij}), \quad (4)$$

Figure 1 shows the temperature-dependent variation of the lattice parameter ***a*** of ordered L12-Cu_3Au binary alloy obtained from the MD using three different potentials for the L12-Cu_3Au binary alloy. According to the MD results obtained from all potentials, it is evident from Figure 1 that there is a discontinuity which is thought to be due to phase transformation of the material. Although the lattice parameter values obtained from all potentials are very close to each other at low temperatures, there are slight differences at higher temperatures. On the other hand, our results are consistent with the previously reported exp.[(a)] [19] and exp.[(b)][20] experimental lattice parameter values, especially our results are closer to the values obtained from exp.[(b)] [20] results. The consistency between the experimental and MD simulation results is a clear indication that all three potentials can accurately identify interatomic interactions in the Cu_3Au system. According to the results of MD simulation, the melting temperature of Cu3Au system under zero pressure has been determined as T_m = 1450 ± 5 K for Q-SC, T_m = 1220 ± 5 K for TB and T_m = 1530 ± 5 K for EAM. When our results are compared with the experimentally determined melting point of 1250K[21], the deviation between our determined melting points and the experimental melting point is 16% for Q-SC, -4% for TB and 22.4% for EAM. These results show that the TB potential function for the model alloy system produces a melting temperature more compatible with the experimental value compared to other potential functions. In addition, the reason why the melting temperature deviates from the experimental values is that the MD cell does not contain any structural defect under initial conditions, and the number of particles used in the study is insufficient.

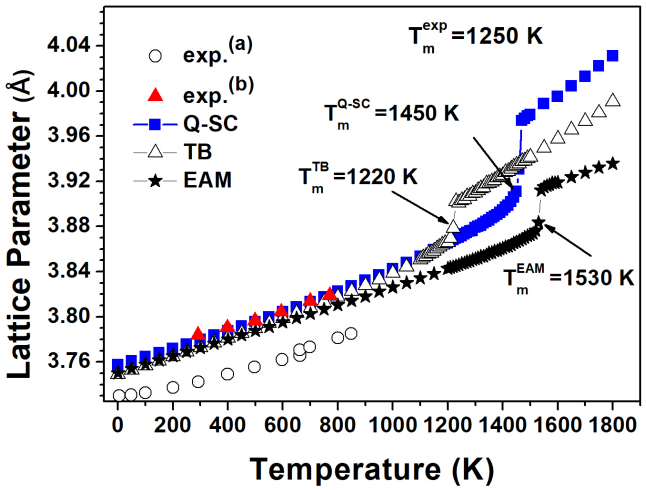

***Fig. 1**. Lattice parameter of Cu_3Au alloy as a function of temperature for all three potentials. The exp.(a) and exp.(b) experimental data have been taken from ref [19] and ref [20], respectively*

Figure 2 shows the final atomic configuration boxes of the system at temperatures of 300K and 1500K, which represent the images obtained using the TB potential. As can be seen from the figure, in 300K there is a uniform distribution between the atoms in the simulation box as in solid systems, whereas in 1500 K the atoms are in a completely random distribution, which is a behavior specific to liquid systems.

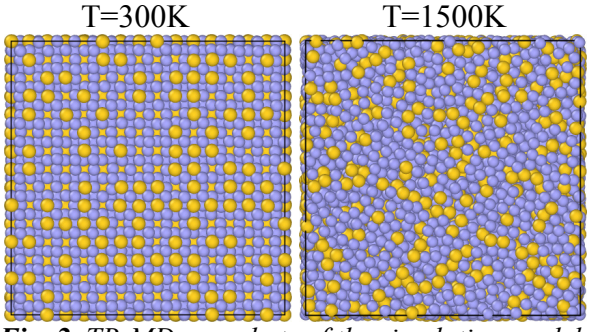

***Fig. 2**. TB-MD snapshots of the simulation models of Cu_3Au alloy at temperatures of 300 K and 1500K. The gray and yellow balls in the simulation box represent Cu and Au atoms, respectively*

The temperature-dependent changes of the specific heat (C_p) curves obtained from QSC-MD, TB-MD and EAM-MD for the Cu_3Au alloy are presented in Figure 3. The C_p values obtained from all potentials exhibit close to each other until their melting point. At low temperatures, the values of Cp are very close to the expected Dulong-Petit value for harmonic solids ($C_p \approx 25$ J mol^{-1} K^{-1}), and these results indicate that these potentials may be successful in explaining the physical properties of the solid system. With increasing temperature, a sudden jump occurred in the C_p curves around the melting points obtained at different points for each potential, which is sudden and sharp jump, indicating that the system is making phase transition from the solid structure to the liquid structure.

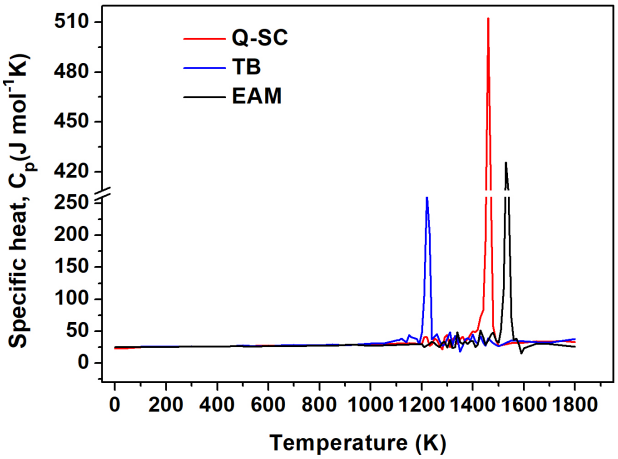

***Fig. 3.** Temperature-related evolution of specific heat curves obtained from Q-SC-MD, TB-MD and EAM-MD during heating*

The pair distribution function (PDF) (or g(r)) is one of the most important structural quantities that characterize a system, particularly for liquids. The PDF for a simulated system can be calculated as follows:

$$g(r) = \frac{V}{4\pi r^2 N^2} \left\langle \sum_i \sum_{i \neq j} \delta(r - r_{ij}) \right\rangle \quad (5)$$

Figures 8 (a-c) show the temperature-dependent evolution of the L12 phase of Cu_3Au alloy under the pressure during the heating process for three different potentials. The g(r) curves calculated at 300K from each of the three potentials show sharp and high peaks representing the solid structure. With the temperature increasing to 900K, different peaks for all potentials gradually begin to disappear and the system tends to liquefy. This tendency to be liquid is more pronounced in the g (r) curves at 1400 K for Q-SC, 1200 K for TB, and 1500 K for EAM. All g(r)'s at 1800 K show a lower first peak and a smoother curve, indicating a property of liquid structures. According to the results of our study, it can be seen that g (r) curves obtained

using three different potentials exhibit similar behaviors.

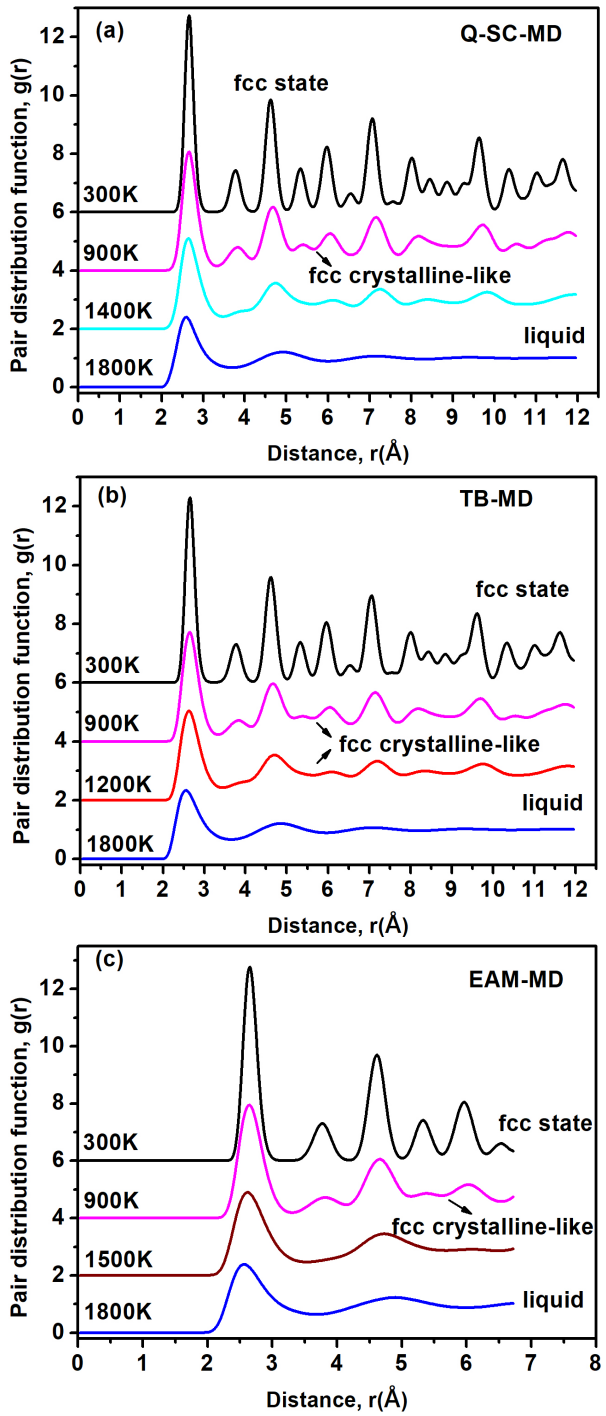

Fig. 3. *g(r) curves at P = 0 for Cu_3Au alloy: solid at T = 300 K, 900 K and 1400 K for Q-SC, 1200 K for TB and 1500 K for EAM, liquid at T = 1800 K, respectively*

CONCLUSION

In summary, in this study, the melting point, specific heat of the system and temperature-dependent changes of the PDF curves were investigated by MD simulations during the heating process by using many body potentials such as Q-SC, TB and EAM for L12-Cu_3Au alloy. The simulated results for all three potentials are consistent with the experimental results in the literature. We have observed that all potential functions used in the study are mostly successful in explaining the structural and physical properties of the system.

REFERENCE

[1] G. De, C.N.R. Rao, Two-Dimensional Au and Au−Cu Alloy Nanocrystals with Orientation in (111) Plane Embedded in Glassy Silica Films ‡, J. Phys. Chem. B. 107 (2003) 13597–13600. doi:10.1021/jp0310091.

[2] L. Battezzati, M. Baricco, M. Belotti, V. Brunella, Microstructure and Thermal Stability of "Nanocrystalline" Electrodeposited Au-Cu Alloys, Mater. Sci. Forum. 360–362 (2001) 253–260. doi:10.4028/www.scientific.net/MSF.360-362.253.

[3] H.R. Zhai, S.M. Zhou, M. Lu, Y.Z. Miao, B.X. Gu, S.L. Zhang, H. Wang, H.B. Huang, The magneto-optical Kerr effect of Fe/Au-Cu and Fe/Al-Cu bilayers, J. Magn. Magn. Mater. 104–107 (1992) 1015–1016. doi:10.1016/0304-8853(92)90467-3.

[4] J. Lohmiller, R. Spolenak, P.A. Gruber, Alloy-dependent deformation behavior of highly ductile nanocrystalline AuCu thin films, Mater. Sci. Eng. A. 595 (2014) 235–240. doi:10.1016/j.msea.2013.12.021.

[5] H. Chabba, M. Lemaallem, A. Derouiche, D. Dafir, Modeling aluminum using molecular dynamics simulation, J. Mater. Environ. Sci. 9 (2018) 93–99. doi:10.26872/jmes.2018.9.1.11.

[6] T. Cagin, Y. Qi, H. Li, Y. Kimura, H. Ikeda, W.L. Johnson, W.A. Goddard, The Quantum Sutton-Chen Many-Body Potential for Properties of fcc Metals, MRS Symp. Ser. 554 (1999) 43.

[7] F. Cleri, V. Rosato, Tight-binding potentials for transition metals and alloys, Phys. Rev. B. 48 (1993) 22–33. doi:10.1103/PhysRevB.48.22.

[8] J. Tersoff, New empirical approach for the structure and energy of covalent systems, 37 (1988).

[9] S. Nosé, A unified formulation of the constant temperature molecular dynamics methods, J. Chem. Phys. 81 (1984) 511–519. doi:10.1063/1.447334.

[10] H. Rafii-Tabar, A.P. Sutton, Long-range

Finnis-Sinclair potentials for f.c.c. metallic alloys, Philos. Mag. Lett. 63 (1991) 217–224. doi:10.1080/09500839108205994.
[11] U. Domekeli, S. Sengul, M. Celtek, C. Canan, The melting mechanism in binary Pd<inf>0.25</inf>Ni<inf>0.75</inf>nanop articles: molecular dynamics simulations, Philos. Mag. 98 (2018). doi:10.1080/14786435.2017.1406671.
[12] F. Cleri, V. Rosato, Tight-binding potentials for transition metals and alloys, Phys. Rev. B. 48 (1993) 22–33. doi:10.1103/PhysRevB.48.22.
[13] M. Celtek, S. Sengul, U. Domekeli, C. Canan, Molecular dynamics study of structure and glass forming ability of Zr70Pd30 alloy, Eur. Phys. J. B. 89 (2016) 1–6. doi:10.1140/epjb/e2016-60694-5.
[14] N.I. Papanicolaou, G.C. Kallinteris, G.A. Evangelakis, D.A. Papaconstantopoulos, M.J. Mehl, Second-moment interatomic potential for Cu-Au alloys based on total-energy calculations and its application to molecular-dynamics simulations, J. Phys. Condens. Matter. 10 (1998) 10979–10990. doi:10.1088/0953-8984/10/48/018.
[15] X.W. Zhou, R.A. Johnson, H.N.G. Wadley, Misfit-energy-increasing dislocations in vapor-deposited CoFe/NiFe multilayers, Phys. Rev. B. 69 (2004) 144113. http://link.aps.org/doi/10.1103/PhysRevB.69.144113.
[16] M.S. Daw, M.I. Baskes, Embedded atom method: derivation and application to impurities,surfaces and other defects in metal, Phsical Rev. B. 29 (1984) 6443–6453.
[17] M. Celtek, S. Sengul, U. Domekeli, Glass formation and structural properties of Zr50Cu50-xAlx bulk metallic glasses investigated by molecular dynamics simulations, Intermetallics. 84 (2017) 62–73. doi:10.1016/j.intermet.2017.01.001.
[18] M. Celtek, S. Sengul, Thermodynamic and dynamical properties and structural evolution of binary Zr 80 Pt 20 metallic liquids and glasses: Molecular dynamics simulations, J. Non. Cryst. Solids. 498 (2018) 32–41. doi:10.1016/j.jnoncrysol.2018.06.003.
[19] G.D. Barrera, R.H. de Tendler, Simulation of metals and alloys using quasi-harmonic lattice dynamics, Comput. Phys. Commun. 105 (1997) 159–168. doi:10.1016/S0010-4655(97)00077-5.
[20] W.B. Pearson, A Handbook of Lattice Spacings and Structures of Metals and Alloys, (Oxford: Pergamon), 1967.
[21] R. Hultgren, D.D. Desai, D.T. Hawkins, Selected Values of Thermodynamic Properties of Binary Alloys, (Metal Park, OH: American Society for Metals), 1973.